applied sciences

MDPI

Article

Damage and Failure of a Column-Supported RC Flat Slab Subjected to Impulsive Loading

David Z. Yankelevsky [1,2,*], Yuri S. Karinski [1] and Vladimir R. Feldgun [1]

[1] National Building Research Institute, Technion–IIT, Technion City, Haifa 3200003, Israel
[2] Faculty of Civil and Environmental Engineering, Technion–IIT, Technion City, Haifa 3200003, Israel
* Correspondence: davidyri@technion.ac.il

Abstract: RC flat slabs supported by an array of columns subjected to the action of impulsive pressure were investigated. The slabs were designed for static loads according to current standards. The dynamic responses of 4 × 4- and 8 × 8-column-supported slabs were similar, as were damage and failure. A simplified model consisting of a tributary area and a central column yielded similar results, demonstrating the accuracy of the simplified model and its reliability. These analyses exhibited modes of damage and failure characterized by large shear distortions in the slab–column connection zone. The rest of the span remained undamaged and in a horizontal position. In all analyses, the slab concrete around the column was fully damaged. The rebars failed within a limited zone at the slab–column connections. The early failure of integrity reinforcement indicated that it could not fulfill its duty; thus, a subsequent progressive collapse scenario was inevitable. All bent-up rebars failed, and their contribution to shear resistance was doubtful. The static analysis was entirely different from the dynamic failure mode. Impulsive loading damage and failure were similar to those in the case of slab-on-slab impact; in both cases, the slab underwent large displacement and severe damage in the narrow slab–column zone, whereas the rest of the slab remained almost completely flat and undamaged.

Keywords: RC flat slabs; multi-span structure; impulsive loading; dynamic response; dynamic punching; slab–column connection

check for updates

Citation: Yankelevsky, D.Z.; Karinski, Y.S.; Feldgun, V.R. Damage and Failure of a Column-Supported RC Flat Slab Subjected to Impulsive Loading. *Appl. Sci.* **2023**, *13*, 1933. https://doi.org/10.3390/app13031933

Academic Editors: Asterios Bakolas and Genevieve Langdon

Received: 5 January 2023
Revised: 21 January 2023
Accepted: 29 January 2023
Published: 2 February 2023

1. Introduction

Reinforced concrete buildings with flat slabs that are supported by columns are very common in residential and office buildings, as their construction is easy and fast and the interior design is free from constraints. A reinforced concrete flat slab supported by columns is characterized by higher shear stresses at its connections with the columns, which sometimes may lead to typical punching shear failure in the slab–column connection zone.

The punching shear problem is well known in flat slabs subjected to static loading and has attracted much research interest over the years [1–7]. Based on the accumulated knowledge, modern standards include specific guidelines to ensure the proper performance of the RC slab–column joint to avoid its damage and failure. The standards instruct to carefully design the slab–column joint to avoid punching shear failure by controlling the slab thickness to provide sufficient shear capacity and by adding special shear reinforcement at the connection zone. Special shear reinforcement may include bent-up omega-shaped rebars crossing the column in the slab–column connection zone or reinforcement links (or shear studs) arranged within the slab in contours around the columns. The standard guidelines are based on the static behavior of flat slabs, and the analysis is carried out accordingly.

Punching shear failure is disastrous, as it disconnects the slab from its supports; the slab then falls downwards and impacts the slab underneath. This local failure may initiate a progressive collapse scenario and turn into global failure [8]. To avoid this catastrophic event, research has expanded to deal with the post-punching shear behavior of flat slabs, aiming at providing an alternative support to the detached slab to arrest the detached slab and prevent its fall, thus preventing failure propagation [1,2,9–11]. This is mainly performed by including special integrity reinforcement, which has shown its efficiency in static load tests [1,3,12–15]. The mechanism of static punching shear failure has been studied widely, both experimentally and analytically [4,5,16–22], and the results of these investigations are implemented in design codes [12–15,23].

The static design of flat slabs is commonly performed using FE linear elastic analysis or, alternatively, simplified hand calculations of continuous beams in both slab directions for representative (column and field) strips of the slab. The analysis results provide the sagging bending moments within the slab span between the columns and the hogging bending moment in the slab–column connection zone and above the columns. Typically, maximum deflections are calculated at midspan. These results are implemented in the design process to assure proper reinforcement design and satisfy the slab performance criteria.

Despite the attention given by different standards to the proper static design of RC flat slabs in general and to avoid punching shear failure in particular, punching shear failure occurs from time to time. There are numerous reasons for the occurrence of such failure under static conditions, such as excessive or unexpected loads; foundation settlement; faulty construction and material properties; material deterioration; combinations of the above; and dynamic loads such as impacts, blasts, and accidental gas explosions.

Relatively to the static behavior of flat slabs, their dynamic behavior and especially their behavior under impact have received only a little attention. Vibration response is commonly solved using similar approaches and tools as in the static loading case. The response of RC flat slabs to extreme dynamic loads has hardly been investigated, although it occurs even in the case described above, where the detached falling slab impacts the slab underneath [24,25]. A limited number of studies refer to the impact punching failure of a flat slab–column connection, mostly with numerical analysis using simplified approaches [26,27] or finite element analysis techniques [28–30]. These studies show that there is a low chance of survivability in the case of progressive collapse due to falling debris. Recently, the impact between two flat RC slabs has been investigated thoroughly [24,25,31,32], and the major failure characteristics have been clarified. The case of flat slabs that are subjected to static loading is characterized by maximum sagging bending moments in the span central zone and hogging maximum bending moments in the connection zone. On the contrary, in the case of impacting slabs, major dynamic punching shear failure occurs where the damage is concentrated in the slab–column connection zone, and no damage is developed along the entire span, which remains almost flat [24,25].

The response of RC flat slabs to high-intensity, short-duration pressure has not gained attention, and the characteristics of damage and failure have not been investigated so far. The major difference between impacting slabs and impulsive pressure loading is that in the first case, the impacted slab is subjected to the interaction pressure of the impacting slabs developed due to the momentum transfer between the slabs, which depends on the slab masses and velocities, whereas in the second case, the pressure–time history is applied over the slab area and its magnitude at any time is predefined and is independent of the slab properties.

The present study aimed at investigating the behavior of a reinforced concrete slab that was designed according to the current design provisions for static loading and was previously investigated for the case of a collapsing slab. It aimed at examining the modes of damage and failure occurring due to the action of impulsive loading and comparing them to the case of slab impact.

Our recent studies on flat slab impact [24,25,32] showed that a realistic model is required to properly simulate the complex behavior of the slab–column connection and its local components, such as longitudinal and shear reinforcement, including its details and locations that take part in the local resistance to the impacting slab. This experience is implemented in the present study, using a similar detailed model which simulates the slab and the rebars. A finite element software AUTODYN [33] that had been used in the case of impacting slabs [24,25,32] is implemented in the present investigation, and the dynamic response analysis of the slabs, accounting for the wave propagation, large strains, and major damage development is carried out. The proposed model has been validated with dynamic low-velocity impact tests on reinforced concrete plates [34,35], and very good correspondence was obtained. The present study refers to an RC flat slab that is supported by an array of columns and subjected to a short-duration constant pressure over the entire slab face area.

2. The RC Flat Slab

Consider an RC flat slab supported by a grid of columns as shown in Figure 1. The slab layout is composed of a 4 m × 4 m square grid of columns supporting 4 m span slabs. A 1.5 kN/m^2 live load that is typical of apartment buildings is considered. According to current design standards [23]. The calculated thickness of the slab according to the serviceability limit state is 14 cm. The slab is supported by 20 cm × 20 cm cross-section columns [23]. The reinforcement is based on the analysis of the slab to static loads according to the current standards [23], using S400 grade steel with a minimum elongation of 12% at fracture and 8% elongation at maximum stress [36].

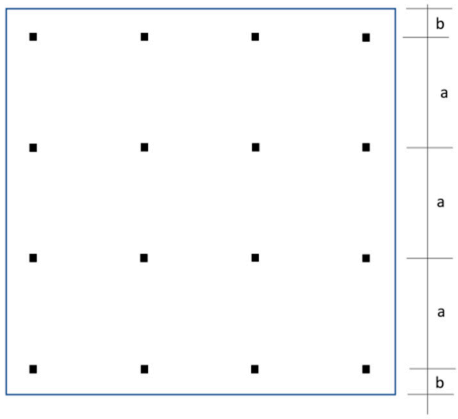

Figure 1. The flat slab layout (a = 4 m, b = 1 m).

A similar slab has been considered in the analysis of a progressive collapse scenario.

The bottom mesh consists of 8 mm diameter rebars at 150 mm spacing in both directions. The top mesh consists of 16 mm bars at 100 mm spacing in the column strips in both directions and 200 mm spacing in other parts of the slab. Two 10 mm diameter 110 cm-length integrity rebars and three 10 mm bent-up bars were added at each connection in each direction. All reinforcement details are presented in [25].

3. The Computational Model

The computational model refers to the entire slab supported by a 4 × 4 columns array (Figure 1). The slab spans are a = 4 m and the cantilevers along the boundaries extend b = 1 m beyond the columns' axis.

An explicit FEM analysis has been carried out using the ANSYS AUTODYN software, implementing a Lagrange (ALE) approach for all elements of the problem [33]. A fine three-dimensional mesh of eight nodes of solid elements was used for the concrete slab domain, and beam elements were used for the reinforcement with joints between concrete and rebar elements.

A perfect bond is assumed between the concrete and steel rebars. The perfect bond is fully justified in the present case, because the results (see below) indicate that major to full damage to the concrete in the connection zone develops shortly after impact. Once the concrete surrounding the rebars is damaged, this damage governs the interaction between the concrete and the rebars, and the perfect bond has no meaning, as the concrete outside the rebar-concrete interface is damaged. This is valid as well for any other assumed bond-slip relationship.

The finite element sizes were determined through a convergence analysis and a fine division of the slab height into 10 elements was adopted. Thus, the solid elements dimensions are 20 mm × 20 mm × 14 mm. These elements were used within an 80 cm × 80 cm central zone around the column axis and gradually larger elements were used at increasing distances from that central zone. The reinforcement element dimensions match the concrete element sizes.

The equation of state (EOS) of 35 MPa concrete is simulated by the P~α model and the deviatoric behavior -by the RHT model. The linear EOS and a bi-linear elastic plastic deviatoric model with failure at a given effective plastic strain are used for the steel rebars. The AUTODYN built-in erosion procedure algorithm is used. An "effective plastic strain" is defined for the concrete and an "on failure" for the steel rebars [33]. The major data used for the concrete and steel models are presented in Table 1; more details are given in [25]. It was shown that the selection of an erosion-effective strain that is lower than "2" (the value that was adopted for the present analysis) is not affecting the solution. Increasing the erosion effective strain beyond "2", yields non-physical results and when this parameter is equal to "2.5" the analysis is terminated prematurely due to the appearance of "corrupted" elements in the slab nearby the column" [25].

Table 1. Material properties for numerical simulations.

Concrete [1]		**Steel** [2]	
Property	**Data**	**Property**	**Data**
Porous density [3]	2314 kg/m^3		
Reference density [3]	2750 kg/m^3	Initial density	7860 kg/m^3
Bulk Modulus	35.27 GPa	Bulk Modulus	167 GPa
Shear Modulus	16.7 GPa	Shear Modulus	77 GPa
Compressive Strength	35 MPa	Yield Stress	400 MPa
Tensile/compressive strengths ratio	0.1	Modulus of linear hardening	667 MPa
Shear/compressive strengths ratio	0.18	Strain Rate constant	0.012
Damage Constant	0.04	Reference strain rate $\dot{\varepsilon}_0$	10^{-4}
Damage Constant	1.00	Plastic strain at failure	8%
Erosion Geometric Strain	2	Erosion Geometric Strain	2

[1]—35 MPa 150 mm-cube uniaxial strength. [2]—type S400. [3]—The porous density is the concrete initial density, whereas the reference density is the density at full compaction which is reached at a very high-pressure level.

4. Impulsive Load over the Entire Slab

4.1. Geometry

In previous studies [25,31,32] that investigated the impact of two slabs, a simple geometrical model was suggested to represent the entire slab and to save considerable computational resources and time for running a single analysis. The simplified model consists of a tributary area a × a (a is the span dimension) having a single central column. The tributary area is subjected to the following boundary conditions representing symmetry and continuity of the complete slab: $\partial w/\partial x = 0$ along the edges x = 0, L and $\partial w/\partial y = 0$ along y = 0, L (where w is the vertical displacement, x is the horizontal coordinate and y is the vertical coordinate in Figure 1). In the present study, the simplified model with the tributary area (Figure 2a) and the entire slab in Figure 1 are analyzed for comparison (Figure 2b). Both calculations refer to the same impulsive loading.

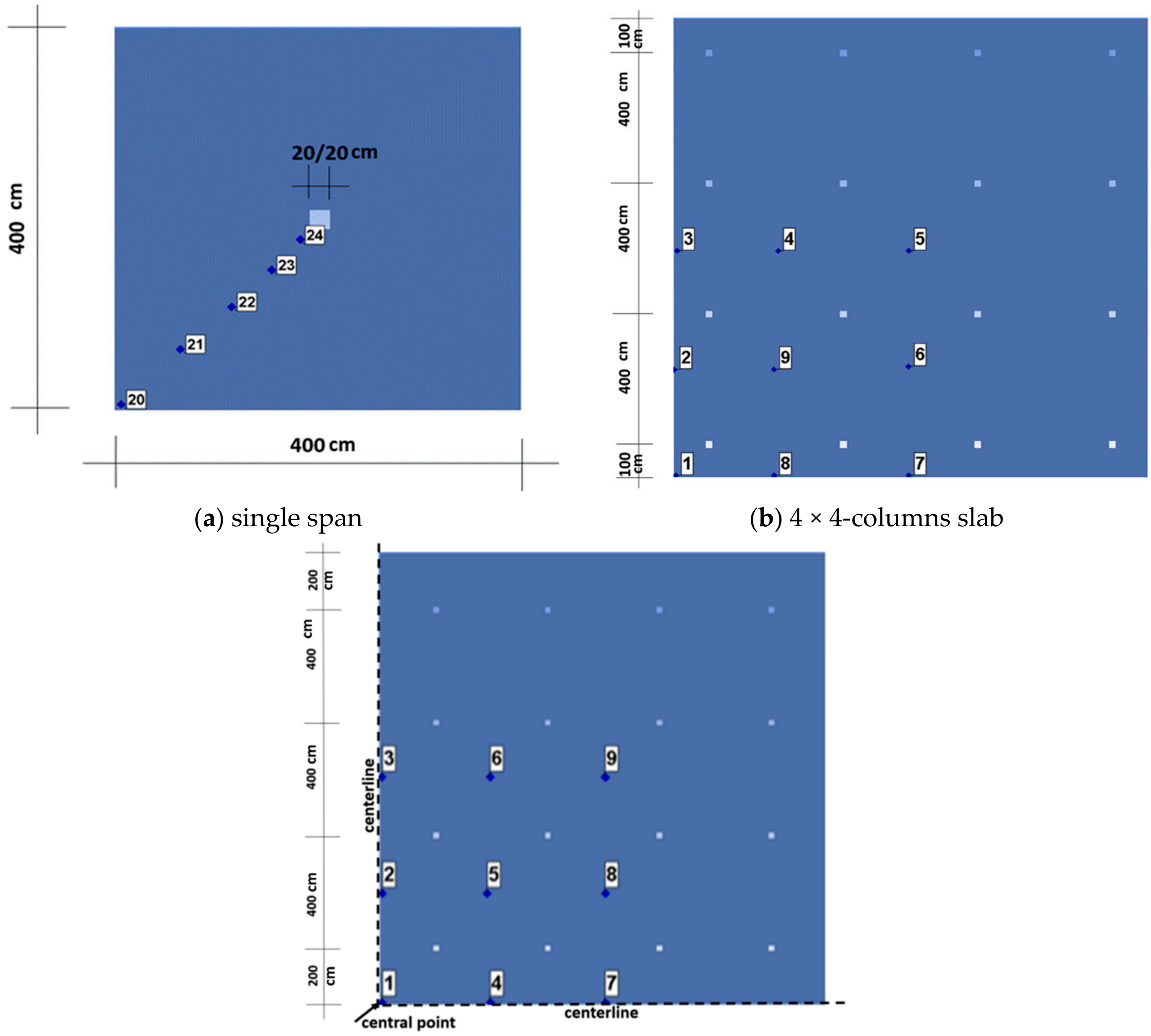

(**a**) single span (**b**) 4 × 4-columns slab

(**c**) columns quarter slab

Figure 2. Gauge locations.

A third analysis is carried out on a multi-span slab (with 2 m cantilevers) supported by 8 × 8 columns (Figure 2c). The third analysis aims at comparing a multi-span (i.e., seven spans) slab response with the response of a slab having a limited number of three spans (Figure 2b), for which the first and central spans may respond somewhat differently. In all three analyses, the slabs are subjected to the same impulsive loading which is uniformly distributed over the entire slab top surface.

From the comparison between these analyses, the accuracy of the simplifying assumption and the reliability of the results obtained from the simplified model and their relevance to the real full-size slab may be concluded. Not less importantly, the response of the slab under the action of an impulsive load is clarified, and its similarity to the case of impacting slabs may be assessed.

Figure 2b is similar to Figure 1 and indicates nine key points at which the slab displacements will be monitored. Points 1 marks the slab corner; points 2, 3, 8, and 7 are laid along the slab cantilever boundaries at mid-distance between column rows; and each of points 4, 5, 6, and 9 are laid at the center of a 400 cm × 400 cm slab. Figure 2a shows the tributary area of the simplified model, and marks five points along half a diagonal (the line connecting points 20 and 24 is the half length of the line between points 5 and 9 in Figure 2b). Point 20 in Figure 2a is identical to points 4, 5, 6, and 9 in Figure 2b. Figure 2c shows a quarter of an 8 × 8 column supported slab, where point 1 is the slab's central point, which is similar to point 5 in Figure 2b.

4.2. Slab Response to Impulsive Loading

4.2.1. The Impulsive Loading

Consider a short-duration impulsive load acting on the entire slab. It is defined by its impulse of 4000 kPa·ms, and by its pressure-time history that is described by a rectangular pulse shape with a pressure of 400 kPa acting during 10 ms, and a zero pressure then after. This impulse intensity has been selected to cause failure and enable evaluation of the slab mode of failure.

4.2.2. Slabs Motion Time-History

Figure 3a shows the velocity-time history for four points in the 4 × 4 columns supported slab. The points are located at the span centers depicted in Figure 2b. The curves describe a very similar response, with a noticeable small difference at point 5 (the slab center) compared to points 4, 6, and 9 which are closer to the slab boundary. Figure 3b shows the velocity-time history for four points in the 8 × 8 columns supported slab. The points are located at the span centers that a close to the center of the slab as depicted in Figure 2c. The curves show identical motion at the four different spans. The signals in Figure 3a,b are very similar, indicating that the 4 m × 4 m slab may represent the response of a similar slab supported by a larger number of columns.

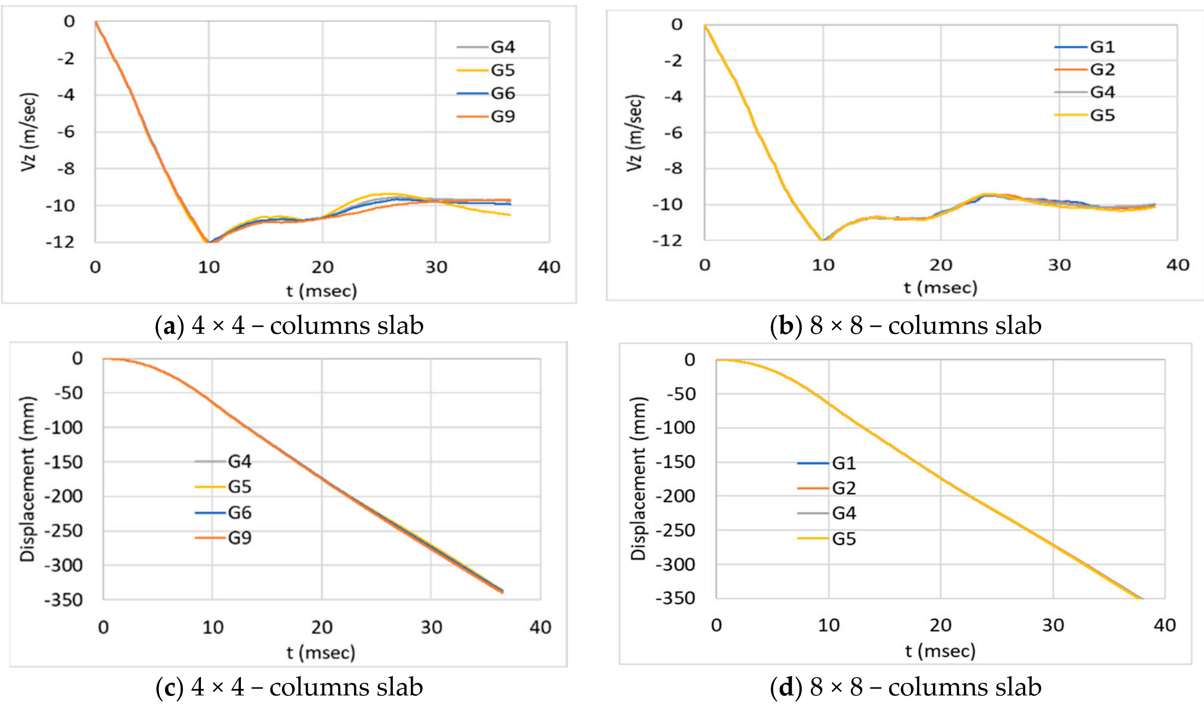

Figure 3. Velocity and displacement time histories at mid-span points.

In both cases, the peak velocity is developed at 10 ms, and attenuates to a lower magnitude permanent velocity within 20–30 ms. This means that the slab has exploited its resistance within that time. Within that duration, the central point displacement exceeds the slab thickness (Figure 3c,d).

Figure 4a indicates that the velocity time histories of the two multi-span slabs are very similar, and the velocity time history of the simplified model only slightly deviates from these curves. The calculated response up to 10 ms is identical and the same peak velocity is reached.

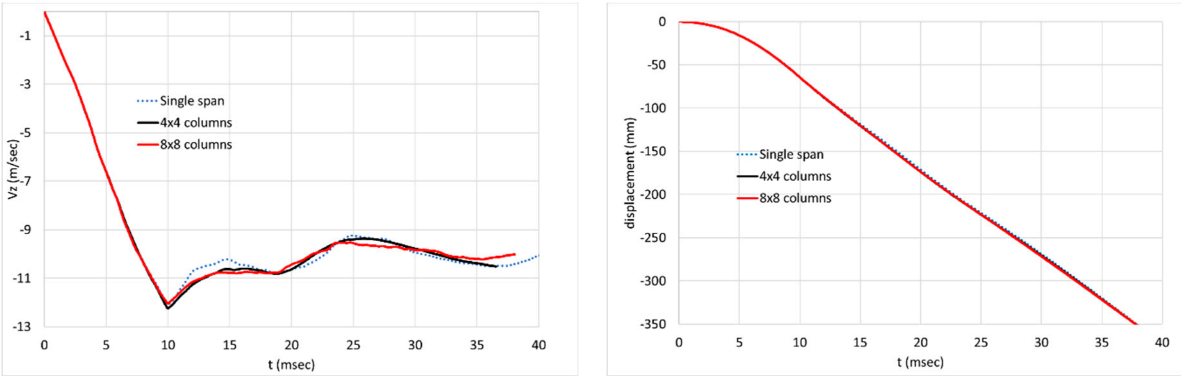

(**a**) velocities (**b**) displacements

Figure 4. Comparison of displacement and velocity time histories.

Then after some deviation from the multi-span curves is observed during the time interval 10–20 ms. All signals reach a similar permanent velocity of ~10.5 m/s. The local minor variations in the velocity-time history are not noticed in the displacement-time history (Figure 4b) where the three curves are identical. This comparison confirms that the simplified model is a reliable representation of the entire slab response under such loading.

4.2.3. Damage and Failure

a. *Damage in the concrete slab*

When the slab velocity approaches a constant magnitude and its displacement is gradually increasing, an ultimate state of failure is reached, where the slab has exploited its resistance capacity, and a failure mechanism is formed. It occurs after ~20 ms, where the central point displacement exceeds the slab thickness. From that instant, the analysis indicates a constant velocity and corresponding linear displacement motion of the slab with respect to the columns and therefore the computation has been terminated after 38 ms.

Figure 5 shows a cross-section of the slab and columns along a typical row of columns after 38 ms, when a central point reaches a displacement of ~350 mm (Figure 4b).

Figure 5a shows the damage along the slab width, through the slab and four columns. The damage scale varies between 0% (in blue) to 100% (in red). Figure 5b shows the damage along the slab width from the slab middle (center line) through the four columns to the right side.

One may see (Figure 5) that the cross-sectional damage patterns in both cases are very similar, with the following major features:

- The damage is concentrated at the slab-column connections. Along the slab spans between the column zones no significant damage is observed.
- The slab damage at the column zone is characterized by 100% damage in the concrete (red color on the damage scale). This means that the concrete is fractured and comminuted and has lost its strength.
- Large shear distortions of the slab are clearly observed in this zone.
- A large displacement is observed between the slab's current position and its original position crossing the column.

The internal spans seem to remain in a horizontal position with minor, almost unnoticeable, curvature.

Comparing the damage in a typical column in Figure 5a,b with the damage in the simplified model is presented in Figure 6 and shows very similar results.

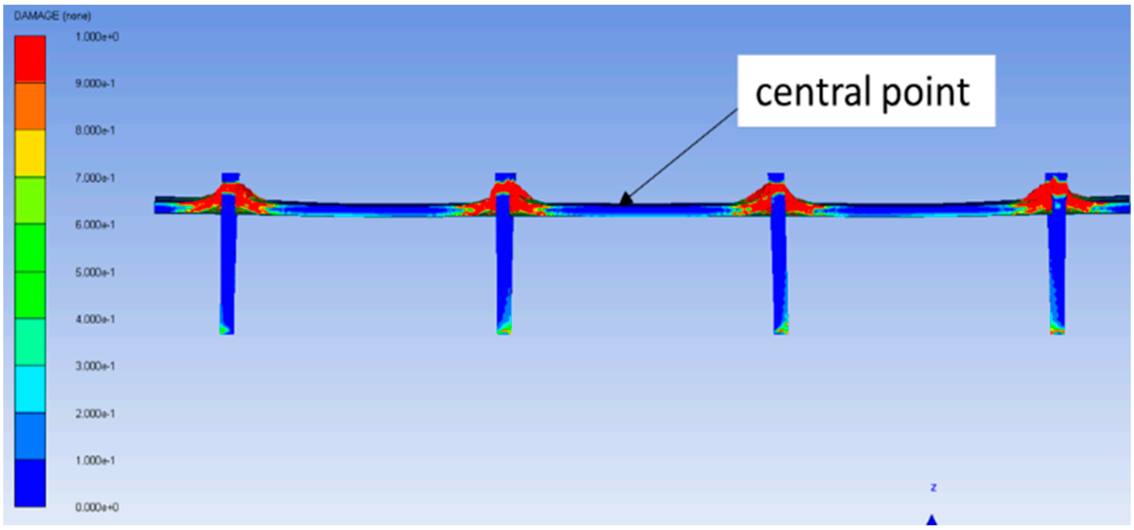

(**a**) width of a 4 × 4 columns slab

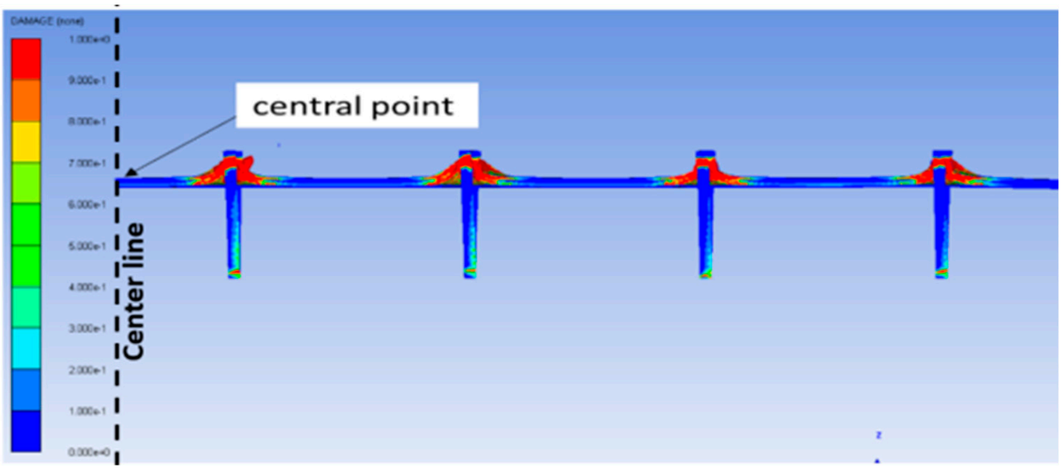

(**b**) half width of an 8 × 8 columns slab

Figure 5. Cross-section (passing through the row of internal columns) after 38 ms.

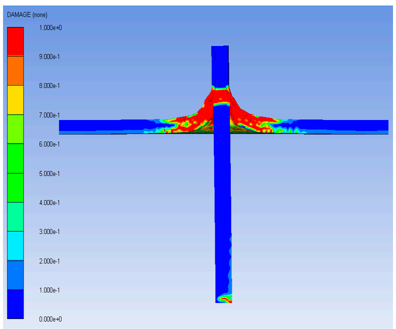

(**a**) single-span slab

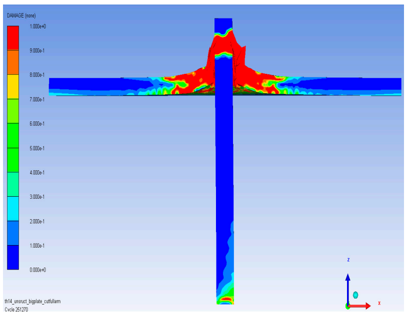

(**b**) 4 × 4-columns slab

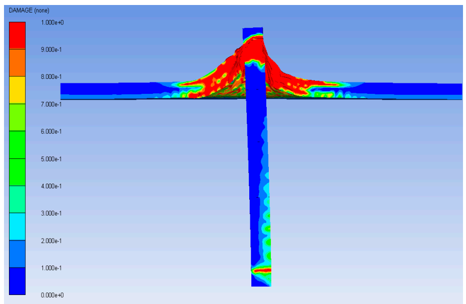

(**c**) 8 × 8-columns slab

Figure 6. Cross-sections of representative slabs.

The top-face damages for the 4 × 4-columns slab (Figure 7a) and the 8 × 8 columns slabs (Figure 7b) are very similar to the damage in the simplified model (Figure 7c).

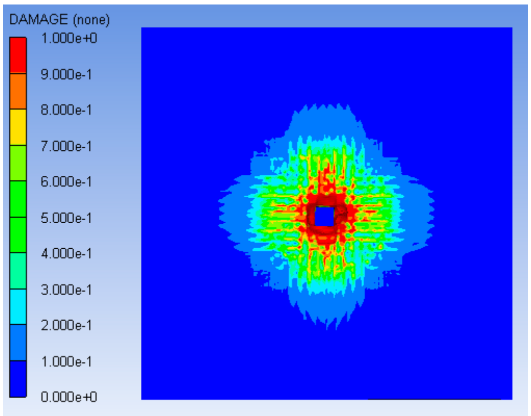

(**a**) 4 × 4−columns slab

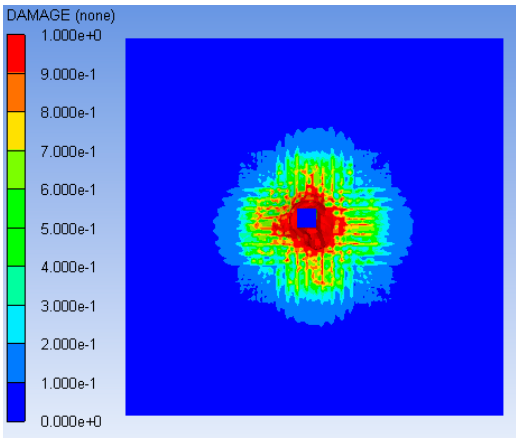

(**b**) 8 × 8−columns slab

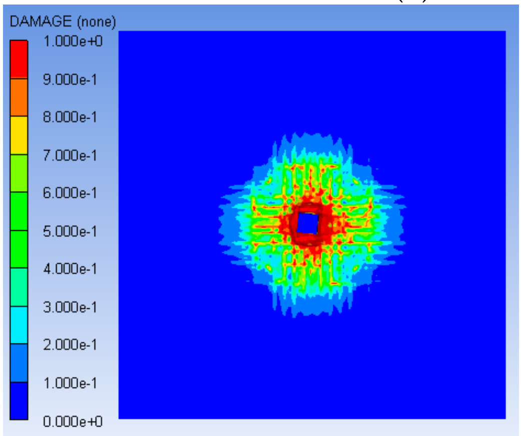

(**c**) single−span slab

Figure 7. Top view damage in the analyzed slabs.

b. *Damage in the reinforcement*

After a complete failure of the slab-column connections is developed, as described above, an examination of the damage and failure of the reinforcement has been carried out. Figure 8 depicts the damage in the top and bottom reinforcement meshes in a column strip along the width of a 4 × 4 column supported slab. Damage is concentrated at limited zones within the slab-column connections only, and the reinforcement remains elastic beyond these zones.

Figure 9 depicts the damage details in the slab-column connection zone. The top rebars in both directions fail close to the column boundary, such that a clear 40 cm× 40 cm square hole is formed through which the column may punch through the top reinforcement.

The mesh deforms upward in its 70 cm× 70 cm central part where a symmetrical bulge is formed around the column axis and an inelastic damage in the rebars is observed (Figure 9a).

The bottom mesh rebars in both directions failed and a clear 30 cm× 30 cm clear hole is formed in the mesh through which the column has punched through (Figure 9b). All integrity rebars fail at cross-sections close to the column boundary. Damage is observed at the rebars and integrity reinforcement with a 90 cm× 90 cm central zone around the column axis.

This failure indicates that the integrity rebars are useless and cannot arrest the slab from falling. The integrity reinforcement cannot fulfill its duty under this loading and a following progressive collapse scenario is inevitable.

The failure of all bent-up rebars is evident (Figure 10) and its contribution to shear resistance is doubtful.

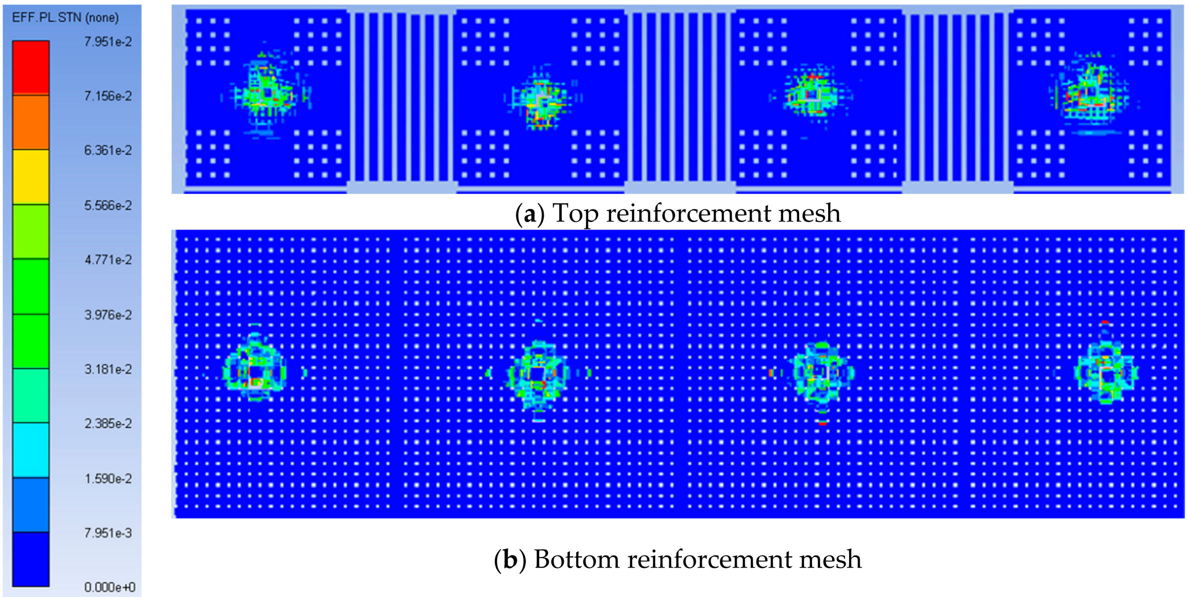

(**a**) Top reinforcement mesh

(**b**) Bottom reinforcement mesh

Figure 8. Damage in slab reinforcement meshes.

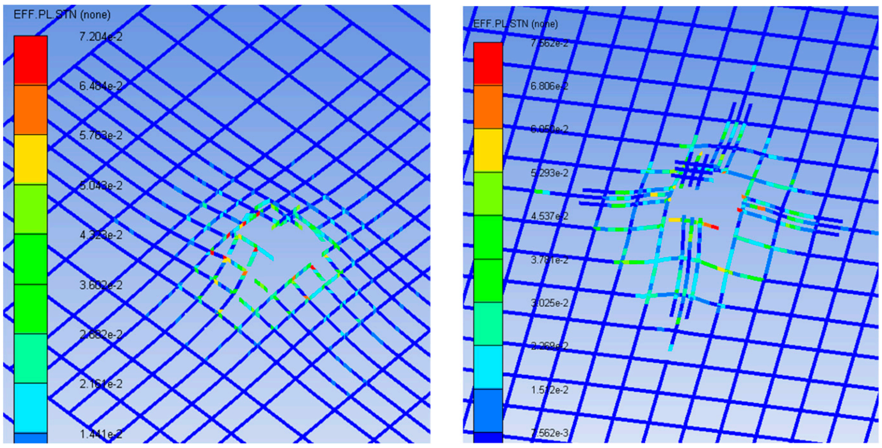

(**a**) Top reinforcement mesh (**b**) Bottom reinforcement mesh

Figure 9. Damage in slab-column zone.

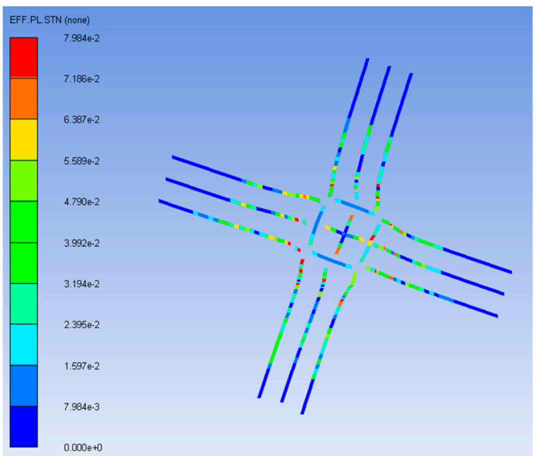

Figure 10. Damage in bent-up rebars.

5. Evaluation of Slab Response to Impulsive Loading

5.1. Impulsive Loading vs. Static Loading

A flat slab supported by columns that are subjected to static loading may be analyzed by a Finite Element discrete method or by calculating the bending of a multi-span beam representing a typical slab strip that is supported by the columns. In both alternatives, the columns strip, indicates the higher bending moments. The bending moment variation is such as that obtained for a multi-span beam showing a maximum hogging bending moment above the column supports and a maximum sagging bending moment at the span central zone. The deflection line shows a variable curvature that is in accordance with the bending moment variation. In a homogeneous beam made of an elastic-plastic material the bending moment magnitudes increase at increasing load intensity, until a plastic bending moment is developed. It develops first above the columns supports and with further increase of the load intensity plastic hinges are formed in the spans central zone and a mechanism is determined where the corresponding load intensity is denoted as the ultimate load. In reinforced concrete elements, the bending moment capacity depends on the sectional properties, on the concrete strength and reinforcement ratio, and on the load level at which a plastic hinge is formed.

The transition from elastic to elastic-plastic behavior is continuous and expected, and the design according to the elastic analysis may indicate the margin of safety for the ultimate load.

This is not the case in the present case, where a slab on columns is considered. The slab design is carried out using the analysis results of an elastic slab supported on columns, which yields the variable bending moments, that determine the reinforcement amount in the slab and their detailing. However, when the slab is subjected to impulsive loading, the failure mechanism turns into a dynamic punching shear failure, that is characterized by severe shear distortions at the slab-column connection zone, accompanied by local reinforcement damage and failure at that zone, whereas the rest of the slab remains almost undamaged. The failure mode is entirely different and cannot be forecasted or extrapolated from the slab analysis and its performance under the design loads. There is no relationship between the elastic-based design and the slab capacity to the impulsive load action. This peculiar situation should be noted, and it deserves special attention in subsequent studies.

5.2. Impulsive Loading vs. Slab-on-Slab Impact

Impulsive loading on a slab is characterized by an independent short-duration pressure-time history which is applied on the slab top surface. This scenario is investigated above, and typical damage and failure results are depicted in Figures 6 and 7.

A slab-on-slab impact is a typical action occurring during a progressive collapse scenario where one slab is falling on top of another slab that is located at a lower level and the intensity of the impact between the slabs depends on the slabs' masses and their velocities. In this case, the implicit interaction pressure and its duration affect the following motion of the impacting slabs. This behavior had been investigated by the authors recently, and typical damage and failure results are depicted in Figure 11.

Comparison of Figures 6, 7 and 11 shows many similarities. In both different loading cases, the slab undergoes large displacements, severe damage is developed at the slab-column zone whereas the rest of the slab remains almost completely flat and undamaged. Therefore, the simplified model composed of a single representing column connected to a tributary area is justified and may represent the entire slab response. This model yields very good results that are in excellent agreement with the full-size slab solution. The analysis results in both cases indicate that the evolution of damage yields a complete failure within a very short duration of ~20 ms.

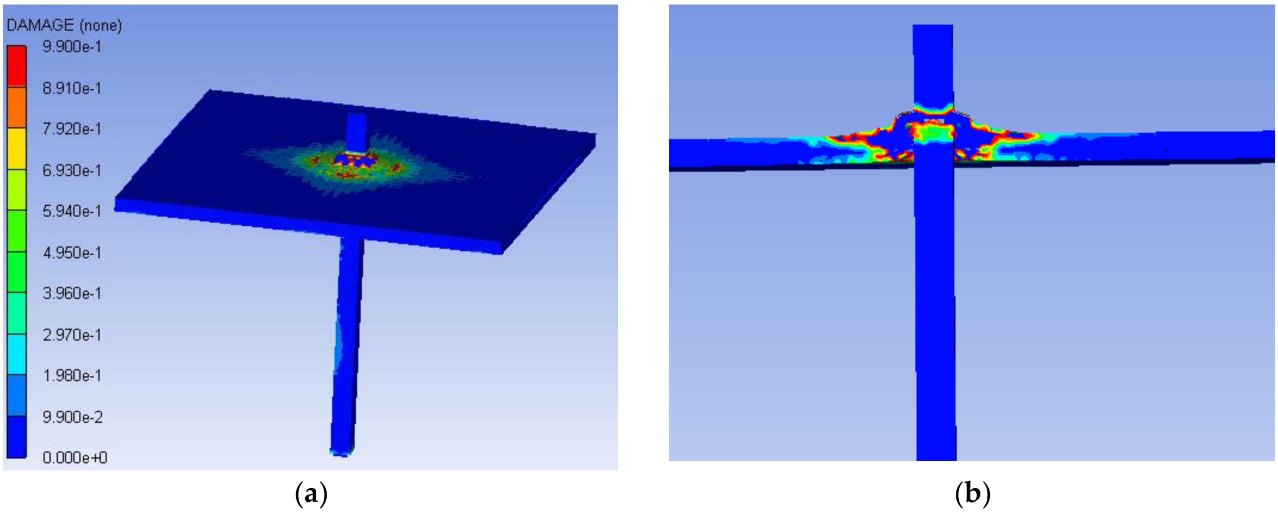

Figure 11. Slab-on-slab damage and failure. (**a**) Top view. (**b**) Cross-section.

6. Conclusions

The present study refers to an RC flat slab that is supported by an array of columns (4 × 4 and 8 × 8) and subjected to a short duration constant pressure. The slab thickness and its reinforcement are designed for static loads according to a current standard. The 35 MPa concrete is simulated by the P~α model for the equation of state and the RHT model for the deviatoric behavior. The linear EOS and a bi-linear elastic plastic deviatoric model with failure at a given effective plastic strain are used for the steel rebars. A simplified model consisting of a tributary area with a span size having a single central column and "symmetry" boundary conditions is used for comparison. Comparison between the full-size slabs' response and the simplified model response demonstrates the accuracy of the simplified model and its reliability for this loading.

All these analyses have clarified the response of the RC flat slab to the action of an impulsive load, and its damage evolution and failure characteristics. It has been shown that the velocity-time histories of the two 4 × 4 and 8 × 8-columns multi-span slabs are very similar, and the velocity-time history of the simplified model only slightly deviates from these curves. The calculated responses up to 10 ms are identical and the same peak and permanent velocities are reached. Furthermore, the local minor variation between the single-span and multi-span slabs is noticed in their velocity-time histories but is not noticed in their displacement-time history. Therefore, the simplified model is a reliable representation of the entire slab response to a uniformly distributed short-duration loading acting on the entire slab. It may provide considerably faster solutions compared to the full-size slab. Examination of the damage map of the full-size slab indicates that damage is developed around each column, whereas the slab domains between these zones remain almost flat and damage free; this justifies the isolation of a tributary area around a column to obtain the calculate the damage-time history, which is similar for every other slab-column connection zone.

The cross-sectional damage patterns in both multi-span slabs are very similar, with the following major features: (1) the damage is concentrated at the slab-column connections, along the slab spans out of the column zones no significant damage is observed; (2) the slab damage at the column zone is characterized by 100% damage in the concrete; (3) large shear distortions of the slab are clearly observed in this zone; (4) a large displacement is observed between the slab current position and its original position crossing the column; (5) the internal spans seem to remain in a horizontal position with minor almost unnoticeable curvature.

The concrete in the connection zone is fully damaged and the slab reinforcement fails at cross-sections that are close to the column circumference. This refers to the top and bottom reinforcement meshes through which the column is punching through, as well as to the integrity reinforcement which fails similarly to the bottom reinforcement. This failure indicates that the integrity rebars are useless and cannot arrest the slab from falling. Therefore, the integrity reinforcement cannot fulfill its expected task to support the failed slab and prevent a progressive collapse. Hence, under this loading, a following progressive collapse scenario is inevitable. The failure of all bent-up rebars indicates their limited role in enhancing shear resistance and their contribution to resisting shear is doubtful.

An interesting observation refers to the difference between the failure mode due to the impulsive loading, which is entirely different from the expected failure under static loading. The static analysis demonstrates the slab bending behavior, with hogging bending moments at the supporting points and sagging bending moments in the central parts of the spans. The expected failure mechanism upon the increase of the static load intensity is the development of plastic moments at these extremal bending moment locations. However, the failure due to the impulsive loading is entirely different and the static design slab of the slab cannot provide suitable resistance to an entirely different mode of damage and failure.

In the author's recent studies on the progressive collapse of flat slabs, the impact between a falling slab and a slab that is located one level below has been investigated. Both impact cases differ in the type of loading: the impulsive load is explicitly given and is independent of the slab and geometry data, whereas the impacting slabs respond to the implicit interaction dynamic pressures which depend on the slab masses and their velocities upon impact. Nevertheless, a comparison between the modes of damage and failure in both cases shows many similarities in concrete and reinforcement damage and failure. In both cases, the impacted slab undergoes large displacements, and severe damage is developed at the narrow slab-column zone whereas the rest of the slab remains almost completely flat and undamaged.

It turns out that the static-loading based structural design of a slab is not suitable to provide the required resistance according to the inspected damage and failure under an impulsive or slab-on-slab impact. This explains why dynamic shear failures occur, and calls for reassessing the design principles to enhance the slabs' resilience.

Author Contributions: Conceptualization, D.Z.Y.; Methodology, D.Z.Y.; Validation, Y.S.K.; Formal analysis, Y.S.K. and V.R.F.; Investigation, D.Z.Y., Y.S.K. and V.R.F.; Supervision, D.Z.Y.; Writing original draft preparation, D.Z.Y.; Writing—review and editing, D.Z.Y., Y.S.K. and V.R.F. All authors have read and agreed to the published version of the manuscript.

Funding: This work was supported by the Israeli Ministry of Construction and Housing and by the Centre for Absorption in Science of the Ministry of Immigrant Absorption and the Committee for Planning and Budgeting of the Council for Higher Education under the framework of the KAMEA Program.

Institutional Review Board Statement: Not applicable.

Informed Consent Statement: Not applicable.

Data Availability Statement: The study did not report any data.

Conflicts of Interest: The authors declare no conflict of interest.

References

1. Ruiz, M.F.; Mirzaei, Y.; Muttoni, A. Post-Punching Behavior of Flat Slabs. *ACI Struct. J.* **2013**, *110*, 801–812.
2. Yi, W.J.; Zhang, F.Z.; Kunnath, S.K. Progressive Collapse Performance of RC Flat Plate Frame Structures. *ASCE J. Struct. Eng.* **2014**, *140*, 04014048. [CrossRef]
3. Wieczorek, B. Idea of a Simplified Model to Determination of the Load Capacity of an Inner Slab-Column Connection after its Punching. In *Procedia Engineering*; Elsevier Ltd.: Amsterdam, The Netherlands, 2013; pp. 126–134.
4. Muttoni, A. Punching Shear Strength of Reinforced Concrete Slabs without Transverse Reinforcement. *ACI Struct. J.* **2008**, *105*, 440–450.
5. Jürgen, E.; Ospina, C.E.; Ruiz, M.F.; Muttoni, A. Punching Shear Capacity of Continuous Slabs. *ACI Struct. J.* **2016**, *113*, 861–872.
6. Broms, C.E. Concrete Flat Slabs and Footings Design Method for Punching and Detailing for Ductility. Ph.D. Thesis, KTH Royal Institute of Technology, Stockholm, Sweden, 2005.
7. Birkle, G.; Dilger, W.H. Influence of Slab Thickness on Punching Shear Strength. *ACI Struct. J.* **2008**, *105*, 180–188.

8. Kiakojouri, F.; De Biagi, V.; Chiaia, B.; Sheidaii, M.R. Strengthening and retrofitting techniques to mitigate progressive collapse: A critical review and future research agenda. *Eng. Struct.* **2022**, *262*, 114274. [CrossRef]
9. Kai, Q.; Bing, L. Strengthening of Multibay Reinforced Concrete Flat Slabs to Mitigate Progressive Collapse. *ASCE J. Struct. Eng.* **2015**, *141*, 04014154.
10. Qian, K.; Bing, L. Strengthening and Retrofitting of RC Flat Slabs to Mitigate Progressive Collapse by Externally Bonded CFRP Laminates. *J. Compos. Constr.* **2013**, *17*, 554–565. [CrossRef]
11. Sasani, M.; Kazemi, A.; Sagiroglu, S.; Forest, S. Progressive Collapse Resistance of an Actual 11-Story Structure Subjected to Severe Initial Damage. *J. Struct. Constr. Eng.* **2011**, *137*, 893–902. [CrossRef]
12. *ACI 318. 318-14*; Building Code Requirements for Structural Concrete and Commentary. American Concrete Institute: Farmington Hills, MI, USA, 2014.
13. *CAN/CSA-A23.3-04*; A National Standard of Canada. A23.3-04 Design of Concrete Structures. Standards Council of Canada: Ottawa, ON, Canada, 2004.
14. *EN 1992-1-1:2004*; Eurocode 2: Design of Concrete Structures—Part 1-1: General Rules and Rules for Buildings. British Standard Institution: London, UK, 2004.
15. *fib Model Code 2010*; Fib Model Code for Concrete Structures. International Federation for Structural Concrete (fib): Lausanne, Switzerland, 2010.
16. Hallgren, M.; Bjerke, M. Non-Linear Finite Element Analyses of Punching Shear Failure of Column Footings. *Cem. Concr. Compos.* **2002**, *24*, 491–496. [CrossRef]
17. Hueste, M.B.D.; Wight, J.K. Nonlinear Punching Shear Failure Model for Interior Slab-Column Connections. *J. Struct. Eng.* **2002**, *125*, 997–1008. [CrossRef]
18. Micallef, K.; Sagaseta, J.; Ruiz, M.F.; Muttoni, A. Assessing Punching Shear Failure in Reinforced Concrete Flat Slabs Subjected to Localised Impact Loading. *Int. J. Impact Eng.* **2014**, *71*, 17–33. [CrossRef]
19. Muttoni, A.; Ruiz, M.F.; Bentz, E.; Foster, S.; Sigrist, V. Background to *fib* Model Code 2010 Shear Provisions—Part II: Punching Shear. *Struct. Concr.* **2013**, *14*, 204–214. [CrossRef]
20. Tetsuya, Y.; Nanni, A.; Endo, K. Punching Shear Resistance of Flat Slabs: Influence of Reinforcement Type and Ratio. *ACI Struct. J.* **1992**, *89*, 555–563.
21. Yankelevsky, D.Z.; Leibowitz, O. Punching Shear in Concrete Slabs. *Int. J. Mech. Sci.* **1999**, *41*, 1–15. [CrossRef]
22. Fraile, D.H.; Setawan, A.; Santos, J.B.; Ruiz, M.F.; Muttoni, A. Punching of Edge Columns with and without Shear Reinforcement: An Experimental Investigation. In Proceedings of the fib International Congress, Oslo, Norway, 12–16 June 2022.
23. *ISO-466*; Israeli Code. 2013, Part 1: Concrete Code: General Principles. Israeli Standards Institute: Tel-Aviv, Israel, 2013.
24. Yankelevsky, D.Z.; Karinski, Y.S.; Feldgun, V.R. Dynamic Punching Shear Failure of a RC Flat Slab-Column Connection under a Collapsing Slab Impact. *Int. J. Impact Eng.* **2020**, *135*, 103401. [CrossRef]
25. Yankelevsky, D.Z.; Karinski, Y.S.; Brodsky, A.; Feldgun, V.R. Evaluation of punching shear design criteria to prevent progressive collapse of RC flat slabs. *Int. J. Prot. Struct.* **2021**, *12*, 174–205. [CrossRef]
26. Olmati, P.; Sagaseta, J.; Cormie, D.; Jones, A.E.K. Simplified Reliability Analysis of Punching in Reinforced Concrete Flat Slab. *Eng. Struct.* **2017**, *130*, 83–98. [CrossRef]
27. Vlassis, A.G.; Izzuddin, B.A.; Elghazouli, A.Y.; Nethercot, D.A. Progressive Collapse of Multi-Storey Buildings Due to Failed Floor Impact. *Eng. Struct.* **2009**, *31*, 1522–1534. [CrossRef]
28. Genikomsou, A.S.; Polak, M.A. Finite Element Analysis of Punching Shear of Concrete Slabs Using Damaged Plasticity Model in ABAQUS. *Eng. Struct.* **2015**, *98*, 38–48. [CrossRef]
29. Terranova, B.; Whittaker, A.; Schwer, L. *Design of Reinforced Concrete Panels for Wind-Borne Missile Impact*; Technical Report MCEER-17-0004; University at Buffalo: Buffalo, NY, USA, 2017.
30. Terranova, B.; Whittaker, A.; Schwer, L. Benchmarking Concrete Material Models Using the SPH Formulation in LS-DYNA. In Proceedings of the 15th International LS-DYNA®Users Conference, Dearborn, MI, USA, 10–12 June 2018.
31. Yankelevsky, D.Z.; Karinski, Y.S.; Brodsky, A.; Feldgun, V.R. Dynamic punching shear of impacting RC flat slabs with drop panels. *Eng. Fail. Anal.* **2021**, *129*, 105682. [CrossRef]
32. Yankelevsky, D.Z.; Karinski, Y.S.; Tsemakh, D.; Feldgun, V.R. From impact of RC flat slabs in a building to its progressive collapse. *Int. J. Prot. Struct.* **2022**, *13*, 439–466. [CrossRef]
33. *Ansys Autodyn*; Theory Manual. Revision 4.3; Century Dynamics: Concord, CA, USA, 2005.
34. Miyamoto, A.; King, M.W.; Fujikake, M. Analysis of Failure Modes for Reinforced Concrete Slabs Under Impulsive Loads. *ACI Struct. J.* **1991**, *88*, 538–545.
35. Bhatti, A.Q.; Norimitsu, K.; Kiang Hwee Tan. Impact Resistant Behaviour of RC Slab Strengthened with FRP Sheet. *Mater. Struct.* **2011**, *44*, 1855–1864. [CrossRef]
36. *ISO 6935-2:2019*; Steel for the Reinforcement of Concrete—Part 2: Ribbed Bars. 3rd Ed, ISO/TC 17/SC 16. International Organization for Standardization: Geneva, Switzerland, 2019.